

Problems of Modeling Diffraction and Interference Processes in Nonlinear and Relaxed Optics

Petro P. Trokhimchuck*

Anatoliy Svidzinskiy Department of Theoretical and Mathematical Physics, Lesya Ukrayinka Eastern European National University, 13 Voly Avenue, 43025, Lutsk, Ukraine.

***Corresponding Author:** Petro P. Trokhimchuck, Anatoliy Svidzinskiy Department of Theoretical and Mathematical Physics, Lesya Ukrayinka Eastern European National University, 13 Voly Avenue, 43025, Lutsk, Ukraine.

Abstract: Diffraction and interference processes in Nonlinear and Relaxed Optics are discussed. Nature and basic peculiarities of formation and development these phenomena are discussed. Influence diffraction and interference processes on the formation various processes of Nonlinear Optics (self-focusing, self-trapping, nonequilibrium gratings, holography and other) is analyzed. The role of diffraction on processes of Relaxed Optics (diffraction layering, irreversible gratings and frozen the proper phenomena of Nonlinear Optics in irradiated matter) is discussed. The corresponding experimental data and models are represented too. Perspective of development and use these methods are analyzed too.

Keywords: Nonlinear Optics, Relaxed Optics, diffraction, interference, gratings, Rayleigh, cascade processes, self-trapping, Cherenkov radiation.

1. INTRODUCTION

The problem of diffraction and self-diffraction processes in Nonlinear Optics (NLO) and Relaxed Optics (RO) has long history [1 – 31]. Roughly speaking NLO phenomena are conducted with RO processes (aging of irradiated materials and basic NLO elements and devices).

The question about nonequilibrium laser-induced diffraction gratings were analyzed in [1]. Diffraction is connected with self-trapping too [1, 11-13]. Self-trapping is result of equivalence self-focusing and diffraction [1].

These problems have large value in RO [1, 11-13]. Methods of RO are used for the creation new laser technologies for the creation nano and microstructures [2-4, 32]. So, laser-induced surface, interferograms may be explained with help Makin plasmon-polariton concept [10]. But microstructure of these interferograms of nano and micro columns can't observe with help of this concept. One of possible mechanism of this phenomenon may be formation of surface diffraction grating. In this case we have two processes: wave processes of creation interferograms and local processes of creation frozen diffractogram, which is modulated by interferograms. This fact may be explained with help physical-chemical cascade theory of excitation proper chemical bonds in the regime of saturation the excitation [4].

For use focused laser radiation in impurity range of absorption spectrum of irradiated matter we can have next scenario [32]. Firstly is diffraction layering; secondly after further focusing nof layeringn irradiation we have generation cascade of Cherenkov radiation [32] (for experimental data< which are represented in [33, 34] 5-stages cascade; thirdly this Cherenkov radiation is caused of creation frozen channels of optical breakdown. In this case we can represent observed experimental data as creation of irreversible diffraction grating too.

The processes of nonequilibrium and irreversible changes in laser-irradiated matter nmay be represented with point of theory of phase transformations. So, basic classical nonlinear optical phenomena may be represented as nonequilibrium second order phase transitions according by H. Haken [35]. The irreversible laser-induced phase transformations have larger spectrum [1, 5, 11-13].The problem of diffusion and self-diffusion processes in Nonlinear and Relaxed Optics wasn't research in whole, therefore this paper allow to represent this problem as autonomous problem

2. EXPERIMENTAL DATA

Interference and diffraction processes are wave processes; therefore we must analyze Nonlinear Optical processes and phenomena according to this fact.

Roughly speaking diffraction gratings are generated in the result of interference various waves on surface or volume of irradiated matter. As example, proper experimental data are represented on Fig. 1 and Fig. 2.

Samples of Ge {111} and Ge {001} i-type single crystals are used in experiment. Nd:YAG laser (wavelength 1,064 μm , duration of pulse 15 ns, pulse rate 12,5 Hz, power $P = 1 \text{ MW}$) was used for the irradiation. The AFM picture of Ge surface after Nd laser irradiation is represented in Fig. 1 [9].

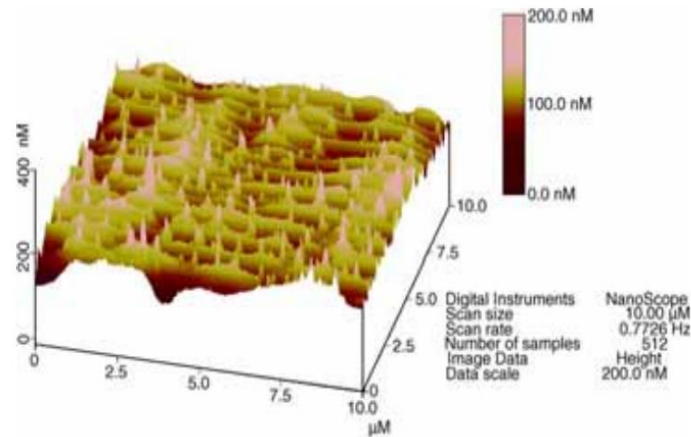


Fig1. Three-dimensional AFM image of nanostructures after Nd:YAG laser irradiation with density of power 28 MW/cm^2 on Ge surface [9]

AFM 3D image of GaAs surface after irradiation serie of pulses by Nd:YAG laser (density of power $I=5,5 \text{ MW}\cdot\text{cm}^{-2}$, $\lambda = 0,532 \mu\text{m}$, $\tau_i = 10 \text{ ns}$) is represented on Fig. 2 [9]. Nanohills have various high and place in the maximums of interferograms.

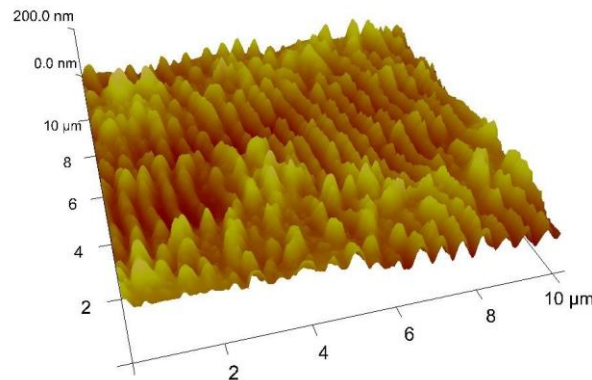


Fig2. AFM 3D image of GaAs surface after irradiation by second harmonic Nd:YAG laser at $I=5,5 \text{ MW}\cdot\text{cm}^{-2}$ [9]

Analogous results were received for the titanium [2]. In report [10] the results of experiments are resulted on the saltatory change of period of remaining surface resonance nanostructures, formed under the action of series of impulses of femtosecond laser radiation on initial polished surface of massive titan. In experiments used radiation of titan-sapphire laser with a central wavelength 800 nm, by a pulsewidth $t = 66 \text{ fs}$, by energy in an impulse about 1 mJ and maximal frequency of pulse-repetition $f=1 \text{ kHz}$.

The massive optically polished plates of titan were used. Typical diameter of area of influence of laser radiation, focused on the surface of sample by a lens, was equaled 0.9 mm. The characteristic density of power of laser radiation on surface of sample was $q \approx 10^{12} \text{ W}/\text{cm}^2$. A radiation was directed on a normal to the surface of sample. The study of character of remaining (stay after a cooling-down of

sample) nanorelief, appearing on the different stages after influence of impulses of radiation, was carried out with the use of scanning electronic microscope (SEM).

The nanorelief of surface, formed at influence of series of impulses of the linear polarized laser radiation, was studied in experiments (Fig. 3). Experiments shown that for series ~ 50-100 pulses of radiation a resonance nanorelief is formed with the wavevector of $\vec{g} \perp \vec{E}$ and period $d_1 \approx 600 \text{ nm}$ (Fig. 3a). Here \vec{E} is a vector of the electric field of laser radiation. At the increase of amount of laser pulses (N), given in the area of irradiation, above $N \geq 200$ in central part of area of irradiation was forming of structures revealed with the period of $d_2 = 300 \text{ nm} = \frac{d_1}{2} = 300 \text{ nm} = d_{1/2}$ (Fig. 3b).

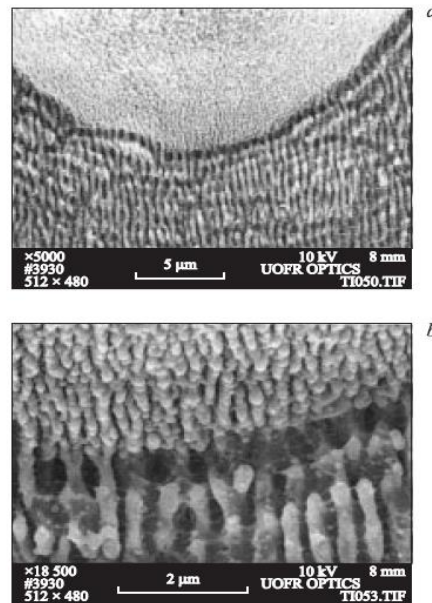


Fig3. SEM pictures of relief of surface of titan, radiation-exposed of the series of pulses of the linear polarized radiation with the density of power $q \approx 10^{12} \text{ W/cm}^2$, $N = 100$: a is an area of periodic nanostructures with the basic period of $d_1 \approx 600 \text{ nm}$; b are structures with the period of $d_2 \approx 300 \text{ nm}$ in central part of area of irradiation and spatial area of bifurcational transition between nanostructures with different periods [4, 10].

A. M. Bonch-Bruevich wanted to use these phenomena for the receiving the reflecting diffraction gratings [10].

These results certify the intrferometric nature of receiving structures. Results, which are represented of Fig. 1 – Fig. 3, are phenomena of RO. But we can assume that creation of nonequilibrium diffractive in NLO has analogous nature.

Influence of diffraction processes on Nonlinear and Relaxed Optical phenomena may be represented on the basis experimental data, which are represented in Fig. 4.

In [33, 34] for minituarization of receiving structures of crystals 4H-SiC were irradiated by pulses of femtosecond laser (duration of pulses 130 fs, wavelength 800 nm, frequency of pulses 1 kHz, density of energy 200-300 nJ/pulse) with help microscope (Fig. 4).

Conditions of irradiation are represented in Fig. 4 ((a), (b)) [33]. Femtosecond laser pulses were irradiated along the lines inside 4H-SiC single crystals at a depth of 30 μm by moving the sample at a scan speed of 10 $\mu\text{m/s}$. The laser beam was irradiated at a right angle to the (0001) surface of the crystal. The irradiated lines were almost parallel to the $[1\bar{1}00]$ direction. A schematic illustration of the laser-irradiated pattern is shown in Fig. 4 (a). The distance between neighboring lines was 20 μm .

Bright-field TEM (transmission electron microscopy) image of the cross section of a line written with a pulse energy of 300 nJ/pulse is shown on Fig. 1 ((c) – (e)) [33].

In contrast to the formation of surface periodical structures three-dimensional periodic structures were obtained in this case. Sectional area of these structures was ~ 22 μm , the depth of ~ 50 μm . As seen from

Fig. 4 (c) we have five stages disordered regions, which are located at a distance from 2 to 4 μm apart vertically [33]. Branches themselves in this case have a thickness from 150 to 300 nm. In this case there are lines in the irradiated nanocavity spherical diameter of from 10 nm to 20 nm. In this case irradiated structures have crystallographic symmetry of the initial structure.

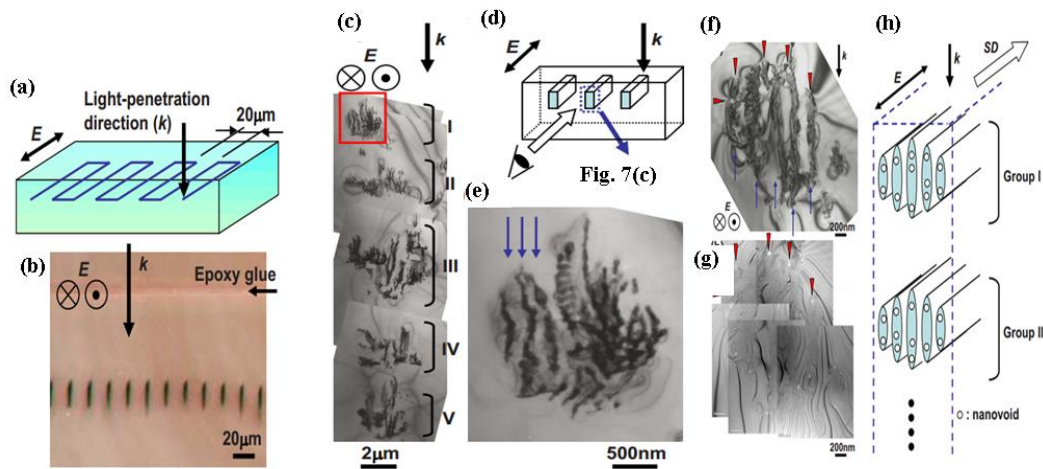


Fig4. (a) Schematic illustration of the laser irradiated pattern. The light propagation direction (k) and electric field (E) are shown. (b) Optical micrograph of the mechanically thinned sample to show cross sections of laser-irradiated lines (200 nJ/pulse). (c) Bright-field TEM image of the cross section of a line written with pulse energy of 300 nJ/pulse. (d) Schematic illustration of a geometric relationship between the irradiated line and the cross-sectional micrograph. (e) Magnified image of a rectangular area in (c). Laser-modified layers with a spacing of 150 nm are indicated by arrows. (f) Bright-field TEM image of a portion of the cross section of a line written with a pulse energy of 200 nJ/pulse. (g) Zero-loss image of a same area as in (f) with nanovoids appearing as bright areas. Correspondence with (f) is found by noting the arrowheads in both micrographs. (h) Schematic illustrations of the microstructure of a laser modified line. Light-propagation direction (k), electric field (E), and scan direction (SD) are shown. Only two groups (groups I and II) of the laser-modified microstructure are drawn [33, 34].

In this case diffraction processes may be generated in two stages: 1 – formation of diffraction rings of focused beams [32] and second – formation of diffracting gratings in the time of redistribution of second-order Cherenkov radiation [32]. Second case is analogous to the creation of self-diffraction gratings in NLO, but for Fig. 4 (c) and Fig. 4 (g) our gratings are limited by Much cone of Cherenkov radiation.

Typical of small-scale filaments at the exit window at a CS_2 created by vself-focusing of multimode laser beam [11] is represented in Fig. 5.

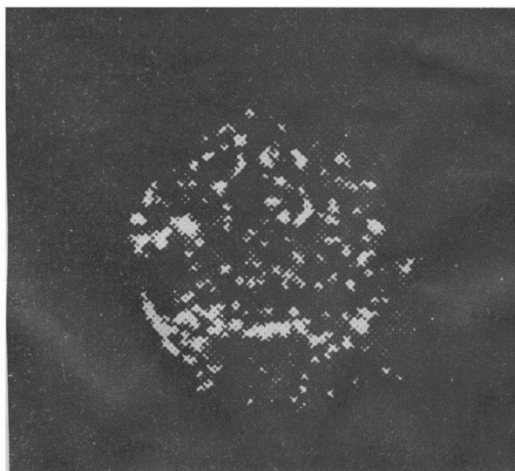


Fig5. Small-scale filaments at the exit window at a CS_2 created by self-focusing of multimode laser beam [11]

The laser-induced filamentation were received in air after irradiation by femtosecond laser pulses (wavelength 800 nm, pulse duration 85 fs, energy 230 mJ and peak power 2,3 TW, i.e. about 700 critical powers according to [36]) (Fig. 6).

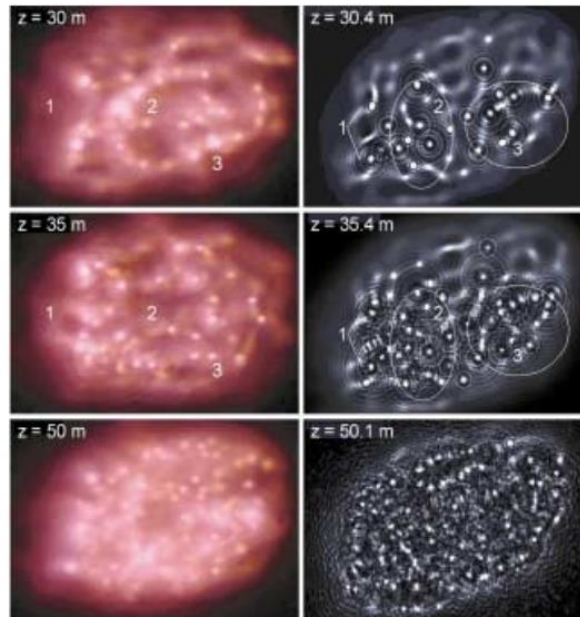


Fig6. Left: Filamentation pattern of the 700 P_{cr} beam delivered by Teramobile laser. Right: Numerical computations [36]. Labels 1-3 spot specific beam zones commented on in the text [36].

A ring-shape zone supports major spots initiated by the highest intense defects of the initial beam (depth $z = 30\text{ m}$). These “hot” spots self-focus more and more over several meters, while they excite secondary smaller-scaled filaments in their vicinity ($z = 35\text{ m}$) [36]. Evacuation of power excess undergone by the primary filaments finally allows transfer of power to the central zone of the beam, which serves as an energy reservoir for exciting new sequences of small spots ($z = 50\text{ m}$). Numerical data were represented for duration of pulse 85 fs and power few terawatt [36]. From these results specific geometrical zones in the beam pattern were selected [36].

Characteristics examples are indicated by labels 1-3 [36]:

- points to a couple of hot couples surviving at further distances;
- indicates in active region of the beam, where intense filaments decay into cell of lesser intensity;
- identifies an area including a cross-wise structure that keeps some filaments robust over 5 m. Condition of receiving self-focusing is next: self-focusing must be more as diffraction [1, 11-13].

Laser generated filaments in solid have white range of radiation spectrum [11-13].

In whole diffraction and interference processes can influence on various proper processes of NLO and RO.

3. MODELING AND DISCUSSIONS

First theory in NLO, which include diffraction, was theory of self-focusing [1]. For the radial symmetry of the profile beam wave equation has next form

$$\left(2ik \frac{\partial}{\partial z} + \nabla_{\perp}^2\right)E = -2k^2 \frac{\Delta n}{n_0} E, \quad (1)$$

where $E = E(r, z, \xi)$ - electrical strength in cylindrical coordinates, Δn - NLO change of refraction index, k – wave number [].

Using $E = Ae^{i\varphi}$ we receive to equations for amplitude A and phase φ

$$k \frac{\partial}{\partial z} A^2 = -\nabla_{\perp} (A^2 \nabla_{\perp} \varphi), \quad (2)$$

$$\frac{\partial}{\partial z} \varphi + \frac{1}{2k} (\nabla_{\perp} \varphi)^2 - k \left(\frac{\nabla_{\perp}^2 A}{k^2 A} + 2 \frac{\Delta n}{n_0} \right) = 0. \quad (3)$$

Equation (2) is energy equation, and (3) – phase equation and determine the trajectory of beam. So far as phase $\varphi(r, z, \xi)$ determine the wave front of beam, then equation (3) is described the vaction of self-focusing, which is represented by term $\frac{\Delta n}{n_0}$, and action of diffraction (term $\frac{\nabla_{\perp}^2 A}{k^2 A}$) []. If in point $z = z_0$ the condition of equilibrium between self-focusing and diffraction is true, than for all r we have next equation

$$\frac{\nabla_{\perp}^2 A}{k^2 A} + 2 \frac{\Delta n}{n_0} = 0, \tag{4}$$

and if for z_0 wave front is planar ($\nabla_{\perp} \varphi = 0$), them from equations (2) and (3) we have $\frac{\partial \varphi}{\partial z} = \frac{\partial A}{\partial z} = 0$ for $z > z_0$. It is case of self-trapping: wave propagates in matter with planar wave front and stable transversal profile. A solution of equation (4) for self-trapping at $\Delta n = n_2 |E|^2$ was received analytically []. But this solution is unstable. Little deviation $A(r, z)$ from self-trapping solution, is caused or self-focusing, or diffraction and or partial self-focusing and partial diffraction solutions. Last case is interesting from point of view of the influence diffraction on NLO processes and phenomena therefore we can receive proper simple equations for other NLO processes.

Lugovoy-Prokhorov theory of moving foci allows explaining the some peculiarities of self-focusing [5, 25]. The layering of laser beam is realized in the direction of irradiation. The results of numerical modeling the dependence of square the dimensionless electrical strength $|X(0, z_1)|^2$ on axis from depth is represented on Fig. 7 [25].

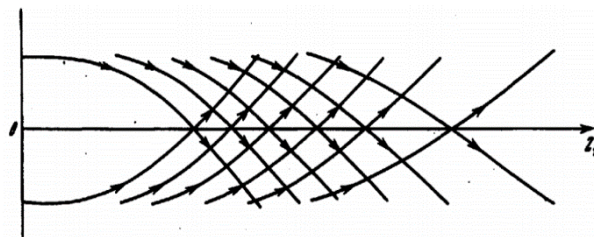


Fig7. Stratification of laser radiation according Lugovoy-Prokhorov theory [25].

Values of parameter N (relation of initial field to critical field) was changed from 1 no 10 [25]. For each value N solution $X(r_1, z_1)$ was received. Herewith $|X(0, z_1)|^2$ were received for few points on axis. For various values of N the layering of initial beam was received [25]. Thus for $N > N_1$ axis field have finite number of intensive maximums. Initial intensity of beam is distributed between maximums, therefore intensity of maximum is received from number of these maximums.

Field analysis outside the axis show that our beam receives the ring structure or other words each maximum is result of focusing proper ring zone [25]. This fact is illustrated on Fig. 7. Distances between maximums is lesser as distance between $z_1 = 0$ and first maximum.

One of the basic conclusions of Lugovoy-Prokhorov model is next: the diffraction stratification of diffraction rings are generated in the process of laser irradiation. This conclusion is similar to basic concept of model, which is based on Rayleigh rings [32]. As for Lugovoy-Prokhorov theory we have that distances between maximums is lesser as distance between $z_1 = 0$ and first maximum (first stage of damage cascade). But in the Lugovoy-Prokhorov theory distances between neighboring maximum (stages of damage cascade) are various, whereas in modified Rayleigh rings model these distances are equal.

The reason for filamentation [13] (formation of filaments 50–80 μm in diameter and with length of several tens of meters in propagation of collimated femtosecond laser pulses in air) is the formation of small-scale self-focusing, which can be caused by the formation of induced diffraction gratings and moving foci [13]. This phenomenon is also associated with the breakdown of air and by its nature is obviously similar to the formation of lightning, only in our case the ionization (breakdown) of the air layer is performed on one side due to multiple narrowly directed photoionization taking into account the processes of reradiation.

In a solid, the filaments are smaller in size, due to the higher density of the matter and are observed in the volume destruction of dielectrics (glass and quartz) [13]. From the physicochemical point of view, these processes can also be described by the methods of relaxed optics [32] (multiphoton ionization in the excitation saturation regime).

Roughly speaking the explanation of experimental data of Fig. 4 (c) is next: the creation cascade of volume destruction is “trace” of moving foci. Each stage of this cascade (Fig. 4 (c)) is result of creation the shock optical breakdown in “Mach cone”. The mechanism of creation new phase of irradiated matter is similar to surface case. In surface case we have generation of surface nano or microcolumn which are perpendicularly oriented to irradiated surface. For volume case (Fig. 4) the nanofilaments are oriented parallel to axe of “Mach cone”. Wave character of these nanofilaments is corresponded to crystal nature of irradiated matter.

Roughly speaking experimental data of Fig 6 are similar to data of Fig. 4 (c), but in this case we have direct multiphoton ionization of volume irradiated matter and next step of its excitation is reradiation of firstly excited air ($z = 30\text{ m}$). This reradiation is source of further excitation air (Fig. 7, $z = 50\text{ m}$) [37]. Laser radiation with wavelength is corresponded first infrared atmospheric “window”, therefore we have large sizes of filaments. Radiation spectra of filaments (from $0,5\ \mu\text{m}$ to $4,5\ \mu\text{m}$) are corresponded to radiation of excited states molecular and atomic nitrogen and oxygen. But energy of ionization of N_2 -molecule is $15,58\text{ eV}$, N -atom – $14,53\text{ eV}$, for molecular and atomic oxygen these values are $12,08\text{ eV}$ and $13,62\text{ eV}$ properly [38].

The estimation of sizes the cascade of volume destructions of Fig. 4 (c) maybe explains in next way [32]. The sizes (diameters) of proper stages d_{nir} of cascade are proportionally to corresponding diffraction diameters d_{ndif}

$$d_{nir} = kd_{ndif}, \tag{5}$$

where k is the proportionality constant.

The diffraction diameters d_{ndif} may be determined with help condition of diffraction-pattern lobes (modified Rayleygh ratio)

$$d_{ndif} = n\lambda. \tag{6}$$

The estimations of diffraction diameters d_{ndif} for $\lambda = 800\text{ nm}$ are represented in Table 1.

Table1 [32].

n	1	2	3	4	5
$d_{ndif}, \text{ nm}$	800	1600	2400	3200	4000

The data of Table 1 for $n=1, 2, 3$ allow to explain of sizes the first three stages of cascade the volume destruction (Fig. 1 (c)). For this case coefficient $k \sim 2$. But for stages 4 and 5 of Fig. 1 (c) our estimations $k_4 \sim 1,2$ and $k_5 = 1$. Various values of coefficients k_i are explained of various conditions of optical breakdown and creation proper phase transformations.

The distance between diffraction spots and proper moving foci may be determined with help next formula

$$l_{nf} = \frac{d_{ndif}}{2 \tan \frac{\varphi}{2}}. \tag{7}$$

These distances for $\varphi_1 = 20^\circ$ and $\varphi_2 = 30^\circ$ are represented in Table 2.

Table2 [32].

n	1	2	3	4	5
$l_{nf}, \text{ nm}$ for $\varphi_1 = 20^\circ$	2269	4538	6807	9076	11345
$l_{nf}, \text{ nm}$ for $\varphi_2 = 30^\circ$	1493	2985	4478	5970	7463

These results are corresponded to Lugovoy-Prokhorov theory too: distance between contiguous elements is smaller as distance between microscopy ocular and first stage of cascade (correlation of this distance is proportional to λ/d) but distance between contiguous elements of cascade is equal and proportional to half wavelength.

Qualitative explanation of development of cascade the destructions may be next. The focus of each diffraction zone (spot) is the founder proper shock optical breakdown. But foci with more high number may placed in the “zone” of influence of previous foci. Therefore only first stage of Fig. 4 (c) is represented pure shock mechanism (Mach cone). Mach cones are characterized the second and third stages of Fig. 4 (c). But its maximums are displaced from center. It may be result if interaction second and third shock waves with previous shock waves: first – for second wave and first and second for third wave. The chock mechanism of destruction certifies a linear direction of optical breakdown. This direction is parallel to direction of shock wave and radiated spectrum is continuum as for Cherenkov radiation and as for observed laser-induced filaments in water and air [13, 32]. Thus basic creator of optical breakdown traces is secondary Cherenkov radiation and shock waves. This radiation is absorbed more effectively as laser radiation and therefore the creation of optical breakdown traces is more effectively as for beginning laser radiation. Cherenkov radiation is laid in self-absorption range of 4H-SiC, but 800 nm radiation – in intrinsic range. For the testing of this hypothesis we must measure the spectrum of secondary radiation. In this case we can use physical-chemical cascade model of excitation the proper chemical bonds of irradiated matter in the regime of saturation the excitation.

We can rough estimate basic peculiarities of energy distribution in Mach cone. Now we estimate the basic energy characteristics of experimental data, where are represented in Fig. 4 (c). Let each stage of cascade has ~200 nanotubes with sizes – $d_{nt} = 20$ nm in diameter and with length $l_{nt} = 500$ nm. General number of these nanotubes is $N_{1snt} \sim 1000$. Its summary volume has value

$$V_{1snt} = N_{1snt} \frac{\pi d_{nt}^2 l_{nt}}{4} = 0,63 \mu m^3. \tag{8}$$

The atom density of 4H-SiC may be determined with help next formula

$$N_a = \frac{\rho N_A}{A}, \tag{9}$$

where ρ – density of semiconductor, N_A – Avogadro number, A – a weight of one gram-atom. For 4H-SiC $N_{aSiC} = 2,4 \cdot 10^{22} \text{ cm}^{-3}$.

Number of atoms in summary volumes of nanotubes is equalled

$$N_{asnt} = N_{aSiC} V_{1snt} = 1,51 \cdot 10^{10}. \tag{10}$$

Energy, which is necessary for the optical breakdown our nanotubes may be determined in next way. Zeitz threshold energy for 4H-SiC is equalled $E_{Zh} \sim 25 \text{ eV}$. Let this value is corresponded to energy of optical breakdown. Therefore summary energy E_{1ob} is equalled

$$E_{1ob} = N_{asnt} \cdot E_{Zh} = 30,2 \text{ nJ}. \tag{11}$$

This value is equalled of 10% from pulse energy. In this case we have more high efficiency of transformation initial radiation to “irreversible” part of Cherenkov radiation. It is result of more intensive excitation comparatively with classical methods of receiving the Cherenkov radiation. In this case we have pure photochemical processes. The experimental data for intrinsic absorption (Fig. 1 – Fig. 3) show that for short pulse regime of irradiation (femtosecond regime) basic processes of destruction the fused silica and calcium fluoride are photochemical (multiphoton absorption in the regime of saturation the excitation). But basic peculiarity of experimental data Fig.1 is transformation the initial laser radiation (wavelength 800 nm) to continuum Cherenkov radiation. From length of optical breakdown in 4Y-SiC we can determine average absorption index of Cherenkov radiation. It is $\sim 10^4 \text{ cm}^{-1}$. This value is corresponded to violet-blue range of absorption spectrum of 4H-SiC. It is corresponded to ultraviolet and violet range of absorption spectrum of 4H-SiC. Analogous pysical-chemical estimations may be made for the data of Fig. 6.

The questions about supercontinuum radiation in the process of femtosecond laser filamentation are discussed in [11 – 13]. In air supercontinuum spectra laid from ultraviolet to infrared ranges of spectra. In whole nonlinear optics of filaments is included the superexpansion of frequency-angle spectrum of

initial pulse, generation of more higher harmonics and terahertz irradiation, pulse compression, optical anisotropy of filament and other nonlinear phenomena [1, 32].

But these questions may be analyzed with point of Cherenkov radiation [39] too. This model may be used for the modification Frank model [39] for the electron “pumping” of Cherenkov radiation on regime of “optical” pumping too. Peculiarities of Cherenkov radiation interference may be represented in next way. We must take into account that sharp directivity of Cherenkov radiation isn’t keep for the zone with sizes lesser as wavelength. Component of frequency ω of light field may be represented as continuous field of stable harmonic oscillator, which are placed on light beam and oriented in the direction of its propagation. In this case oscillators may be have polarized electrical moment p_ω

$$p_\omega = \frac{e}{\pi\omega} \cosh \omega(t - \tau) dl, \tag{12}$$

where e – electron charge, t – time, τ – lifetime of light-induced electron excitation. Field of light beam is sum of all oscillators. As result for frequency $\omega = 2\pi c/n\lambda$ we have amplitude of this field in point of observation, which is placed from point of light excitation ((absorption proper photon) in distance $R \gg l$, is equaled

$$A = A_0 \frac{\sinh \theta}{R} \frac{\sinh \left[\frac{\pi l}{\beta n \lambda} (1 - \beta n \cosh \theta) \right]}{1 - \beta n \cosh \theta}, \tag{13}$$

where λ – wavelength in matter; θ is angle between with beam, which is directed in point of observation, and our beam. Phase is equaled of wave phase oscillator, which is place in the middle point of observed beam.

Now we’ll be observe only excitation with value more as phase speed of light in matter

$$\beta n(\omega) > 1, \tag{14}$$

This condition is necessary for Cherenkov radiation [39]. In addition, we suspect that l is length of light source (size of proper zone of photon scattering) in light direction and is lesser as length of light beam.

These results are true for $l < \lambda$. So according to formula (13) we see that for $l \ll \lambda/2$ field is equaled to field of point dipole, which is oriented along light beam. Therefore for lighting volume, which is smaller as wavelength radiation isn’t differenced from dipole radiation. Only for $l \geq \lambda$ characteristic direction of radiation is arisen. Therefore only for this case (especially for strong divergent beams) we could expect the decreasing of interference property of Cherenkov radiation. But Alentsev researches [38] shown that for the conditions of receiving the interference of dipole radiation the existing of directivity isn’t prevented to interference of Cherenkov radiation.

In whole for Cherenkov radiation in dependence from selection the light beams increasing of zone of light scattering can decrease the interference ability with various speeds (less or more) as for standard radiators.

Let a and b – directions of interference beams from source, which has center in point O (Fig. 8). Let angle between beams a and b is equaled 2φ . Now we consider an interference light of elementary coherent radiators, which are homogeneously distribute on the length l , that find between planes $x = \frac{1}{2}x_0$ and $x = -\frac{1}{2}x_0$. In this case optical path difference for beams are parallel to a and b for any radiator is determined as $2x \sinh \varphi$. Let distance between planes, which are limited the length l , is equaled

$$x_0 = \frac{\lambda}{k \sinh \varphi}, \tag{15}$$

where k is variable, which is determined the quantity x_0 .

Then $\frac{\lambda}{k}$ is equaled by maximal change of optical path difference for radiators, which are placed on opposite ends of l . Interference is maximal for $k \gg 1$ and may be equal to zero for $k = 1$. This dependence from k is identical for each segment, which is placed between planes $x = \frac{1}{2}x_0$ and $x = -\frac{1}{2}x_0$. Thus for observation the interference angularly 2φ for any incoherent light sources is possible for $k \leq 1$.

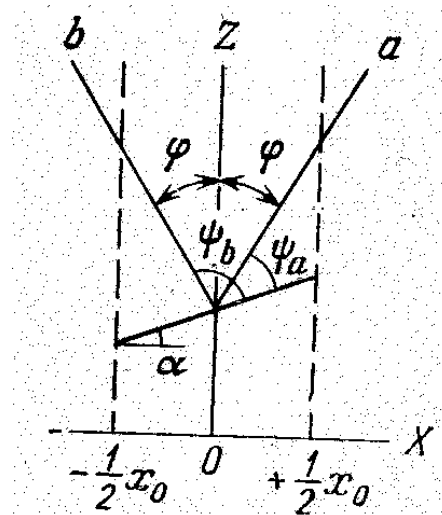


Fig8. To explanation the interference for the divergent beams [39]

Another result we have for the Cherenkov radiation. Let segment of line l is equal the light beam and α – angle between light beam and X-axis. Then optical length of our beam is equaled

$$l = \frac{x_0}{\cosh \alpha} = \frac{\lambda}{k \sinh \varphi \cosh \alpha}. \quad (16)$$

For large value l formula (13) has maximal value for angle θ_ω , which is determined from condition

$$\cosh \theta_\omega = \frac{1}{\beta n(\omega)}. \quad (17)$$

Amplitude is decreased to zero for the increasing the angle from θ_ω to θ_2 or for decreasing from θ_ω to θ_1 . With help formulas (13) and (16) we can determine angles θ_2 and θ_1 .

$$\cosh \theta_2 = \frac{1}{\beta n} - 2k \sinh \varphi \sinh \alpha, \quad (18)$$

$$\cosh \theta_1 = \frac{1}{\beta n} + 2k \sinh \varphi \sinh \alpha. \quad (19)$$

Width of basic diffraction maximum is equaled

$$\cosh \theta_1 - \cosh \theta_2 = \frac{\lambda}{2}. \quad (20)$$

Width of diffraction maximum must be equal or smaller as θ_ω .

Let angles between basic beam and beams a and b are equaled ψ_a and ψ_b properly. Then

$$\cosh \psi_a = \sinh \varphi \cosh \alpha + \cosh \varphi \cosh \gamma, \quad (21)$$

$$\cosh \psi_b = -\sinh \varphi \cosh \alpha + \cosh \varphi \cosh \gamma, \quad (22)$$

where γ is angle between basic light beam and Z-axis.

Interference was observed if angles ψ_a and ψ_b are placed in region of basic maximum of radiation

$$\cosh \theta_2 < (\cosh \psi_a, \cosh \psi_b) < \cosh \theta_1. \quad (23)$$

The inequations (23) are true for $k > 1$ and for $k = 1$. Let direction of general light beam, that $\theta_\omega < \psi_a < \theta_1$; then for $k = 1$

$$\frac{1}{\beta n} < \sinh \varphi \cosh \alpha + \cosh \varphi \cosh \gamma < \frac{1}{\beta n} + 2 \sinh \varphi \cosh \alpha. \quad (24)$$

If subtract from all parts of (24) term $2 \sinh \varphi \cosh \alpha$ then we have

$$\frac{1}{\beta n} - 2 \sinh \varphi \cosh \alpha < -\sinh \varphi \cosh \alpha + \cosh \varphi \cosh \gamma < \frac{1}{\beta n}, \quad (25)$$

or $\theta_2 < \psi_b < \theta_\omega$, notably it lay in the region of basic maximum. Notably in this case interference isn't equal zero even for $k = 1$. If we select direction of general optical beam with condition $\theta_\omega < \psi_a < \theta_2$ for $k = 1$, then ψ_b will be placed in the interior of incidental maximum with negative amplitude (see (13)). For this beam interference is zero for $k = 1$. Thus dependence the interference from length of light source for Cherenkov radiation is another than in standard case and depend from direction the beam propagation.

Cherenkov radiation has next peculiarity. We know fact that induced radiators give possibility to receive two coherent light sources. This fact is used for the standard interference [39]. Analogous phenomenon must be observed for Cherenkov radiation too. If we transmit light beam through two little volumes of similar matter, then we receive two coherent sources. This property is characterized for any wavelength of continuous Cherenkov spectrum [39]. Therefore interference for Cherenkov radiation have broad spectral region [39].

In whole microscopic mechanism of laser-induced Cherenkov radiation may be represented as nonequilibrium spectrum of all possible Nonlinear Optical phenomena in the local points of propagation the laser beam. It may be Raman and Brillouin scattering, up- and down-conversion, generation of harmonics and various interference of these processes and phenomena, which are generated the continuous spectrum from ultraviolet to infrared regions.

Cherenkov radiation with optical pumping may be represented as Nonlinear Optical process with speed is less as light phase speed in irradiated matter. In this case phase speed in matter has physical nature: it is the electromagnetic speed of "collective" motion the charge particles or charge in matter. Therefore in local scale we have Nonlinear Optical processes, which are modulated of the Mach cone the Cherenkov radiation (Fig. 4 (c)). It allow add the Nils and Aage Bohrs theory about microscopic mechanism of Cherenkov radiation [40].

In solid this spectrum must be displaced to ultraviolet range? Therefore our traces of filaments have more little length as in water or air [13, 32]. Basis cause of this fact is more density of solid and more intensive light absorption. But in the liquid and air the direct optical breakdown is realized and these types of matter have more "soft" relaxation as solid. And processes of multiphoton ionization in the regime of self-focusing are more slowly as in solid. Continuum spectrum of filaments in this case are corresponded to the renewal disrupting chemical bonds and electronic states of irradiated molecules and atoms.

Experimertal data of Fig. 1 – Fig. 3 and Fig. 5 may be explain on the basis the two-dimensional interference of various waves or polariton-plasmon according by V. Makin [10]. Maxima of these interferograms are sources of more intensive ionization of irradiated matter and concomitant processes of phase transformations (Fig. 1 – Fig. 3) or radiation (Fig. 5).

As we see sources of Relaxed Optical processes are Optical and Nonlinear Optical processes and phenomena.

Thus short system analysis of basic peculiarities of diffraction and interference processes and phenomena in Nonlinear and Relaxed Optics is represented and discussed.

4. CONCLUSION

1. Problems of creation the surface interference and diffraction structures are discussed.
2. The role of chock processes for the creation laser-induced structures is observed.

3. Model of Rayleigh rings are used for the explanation the creation the cascade of volume destruction 4H-SiC. This model is added to Lugovoy-Prokhorov model of moving foci.
4. Modified Rayleigh model was used for the estimations the sizes and form of nanovoids.
5. Was shown that physical-chemical cascade model of saturation the proper types and number chemical bonds in the regime of saturation the excitation may be used for the explanation surface and volume laser-induced phase transformation.
6. Was show that Cherenkov radiation was generated in the result of diffraction stratification of focused laser beam in irradiated matter (4H-SiC).
7. Microstructure of each term of cascade may be explained as result of interference Cherenkov radiation.
8. Modified I. Frank theory of interference Cherenkov radiation was used for the “optical” regime of generation the Cherenkov radiation.
9. Basic peculiarities of interference Cherenkov radiation are discussed.

ACNOWLEDGEMENT

I would like to express my gratitude to M. Romanyuk, Ya. Dovhyy, M. Pidzyraylo, L. Laz'ko, A. Tsaryk, L. Lutsiv-Shumskiy, V. Melnichak, V. Peretyatko, A. Gorchakov, V. Chernyshov, P. Danylchenko, I. Stoyanova, V. Antonov-Romanovskiy, I. Frank, P. Cherenkov, V. Vinetskiy, A. Prykarpatskiy, L. Muravskiy, V. Yurevich, A. Golubkov, V. Sokolov and E. Katz for discussions various questions of the theory diffraction and interference and nature of Cherenkov radiation.

Author wishes to thank by O. Viligurskiy and D. Shvalikovskiy for the help in the preparation this paper.

REFERENCES

- [1] Shen Y. R. (1989) Principles of nonlinear optics, Nauka, Moscow (In Russian)
- [2] Trokhimchuck P. P. (2018) Problems of modeling the phase transformations in Nonlinear and Relaxed Optics (review). IJERD, Vol.14, Is.2, 48-61.
- [3] Trokhimchuck P. P. (2015) Relaxed Optics: Necessity of Creation and Problems of Development. IJARPS, Vol. 2 , Is. 3, 22-33
- [4] Trokhimchuck P. P. (2016) Relaxed Optics: Realities and Perspectives, Lambert Academic Press, Saarbrücken
- [5] Self-Focusing: Past and Present. (2009) Eds. R.W.Boyd, S.G. Lukishova, Y.-R. Shen, Springer Series: Topics in Applied Physics , Vol. 114, New York, Springer.
- [6] Rayleigh (J. W. Strutt). (2009). Wave theory of light, URSO, Moscow (In Russian)
- [7] Chiao R. Y., Kelley P. L., Carmire E. (1966) Stimulated four-photon interaction and its influence on stimulated Rayleigh-wing scattering. Phys. Rev. Lett, vol. 17, is, 22, 1158 – 1161.
- [8] Vinetskiy V. L., Kughtarev N. V., Odulov C. G., Soskin M. S. (1979) Dynamical self-diffraction of coherence light beam. Advanced in Physical Science, Vol. 129, Is. 1, 113 – 137. (In Russian)
- [9] Medvid' A. (2010) Nano-cones Formed on a Surface of Semiconductors by Laser Radiation: Technology, Model and Properties/ Nanowires Science and Technology, ed. Nicoletta Lupu. – Vukovar: Inech, 61–82.
- [10] Makin V.S. Regularities of creation of ordering micro- and nanostructures in condensed matter for laser excitation of mode of surface polaritons. D.Sc. Thesis, Saint-Petersburg, Russia: State University of Informative Technologies, Mechanics and Optics, 2013. (In Russian)
- [11] Shen Y. R. (1975) Self-focusing: experimental, Progr. Quant. Electr., Vol. 4, 1-34
- [12] Murburger J. H. (1975) Self-focusing: theory. Progr. Quant. Electr., Vol. 4, 1975, 35-110.
- [13] Chekalin S. V., Kandidov V. P. (2013) From Self-Focusing Light Beams to Femtosecond Laser Pulse Filamentation, Advanced in Physical Science, Vol. 56, Is.2, 133-152. (in Russian)
- [14] Kughtarev N. V., Dovhalenko G. E. (1983) Diffraction gyration waves in gyrotropy crystals. Preprint of Physical Institut of Academy Science of Ukraine, Kiyv, (in Russian)
- [15] Dyshko A. L., Lugovoy V. N., Prokhorov A. M. (1967) Self-focusing of intensive light beams, Letters of Journal of Theoretical and Mathematical Physics, Vol. 6, Is. 5, 655-659 (In Russian)
- [16] Dzedolik I. V. (2007) Polaritons in optical fibers and dielectric resonators. DIAYPI, Simferopol (in Russian)
- [17] Kurylyak D. B., Nazarchuk Z. T. (2006) Analytical-numerical methods of diffraction theory of electromagnetic waves. Naukova Dumka, Kyiv (In Ukrainian)

- [18] Cowley J. (1975) Diffraction Physics, North-Holland Publishing Company – Amsterdam, Oxford @ American Elsevier Publishing Company Inc. – New York
- [19] Gorelik G. S. (1959) Oscillations and Waves. Introduction to Acoustic, Radiophysics and Optics, Nauka, Moscow (In Russian)
- [20] Trokhimchuck P. P. (2019) Some Problems of Modeling the Shock Processes of Relaxed Optics. Proc. 3-d Intern. Conf. “Actual Problems of Fundamental Science”, Lutsk – Svitvaz’, June 01 – 05, 2019., Vezha-Print, Lutsk, 125-128
- [21] Brekhovskikh L. M. (1973) Waves in Layering Matter, Nauka, Moscow (In Russian)
- [22] Felsen L. B., Marcuvitz (1973) Radiation and Scattering of Waves, vol. 1, Prentice Hall, Englewood Cliffs, New Jersey
- [23] Felsen L. B., Marcuvitz (1973) Radiation and Scattering of Waves, vol. 2, Prentice Hall, Englewood Cliffs, New Jersey
- [24] Ginzburg V. L. (1960) A Propagation the Electromagnetic Waves in Plasma, Nauka, Moscow (In Russian)
- [25] von Hönl H., Maue A. W., Westfahl K. (1961) Theorie der Beugung, Springer Verlag, Berlin - Göttingen – Heidelberg
- [26] Kanevskiy I. N. (1977) Focusing of Sonic and Supersonic waves, Nauka, Moscow (In Russian)
- [27] Vinogradova M. B., Rudenko O. V., Sukhorukov A. P. (1970) Nauka, Waves Theory, Moscow (In Russian)
- [28] Potekhin A. I. (1948) Some problems of the Diffraction Theory the Electromagnetic Waves, Sovetskoye Radio, Moscow (In Russian)
- [29] Pain H. J. (1976) The Physics of Vibrations and Waves, John Willey and Sons, LTD, London – New York – Sydney – Toronto
- [30] Morze F. (1949) Vibrations and Sound, GITTL, Moscow – Leningrad (In Russian)
- [31] Chiao R. Y., Carmire E., Townes C. H. (1964) Self-trapping of Optical Beams, Phys. Rev. Lett., Vol. 13, No. 15, 479-482.
- [32] Trokhimchuck P. P. (2018) Some Problems of Modeling Volume Processes of Relaxed Optics, IJARPS, Vol. 5, Is.11, 1-14
- [33] Okada T., Tomita T., Matsuo S., Hashimoto S., Ishida Y., Kiyama S., Takahashi T. (2009) Formation of periodic strain layers associated with nanovoids inside a silicon carbide single crystal induced by femtosecond laser irradiation. J. Appl. Phys., Vol. 106, p.054307, – 5 p.`
- [34] Okada T., Tomita T., Matsuo S., Hashimoto S., Kashino R., Ito T. (2012) Formation of nanovoids in femtosecond laser irradiated single crystal silicon carbide. Material Science Forum, Vol. 725, 19 – 22.
- [35] Haken H. (1980) Synergetics, Mir, Moscow (In Russian)
- [36] Berge L., Skupin S., Lederer F., Mejean G., Yu J., Kasparian J., Salmon E., Wolf J. P., Rodrigues M., Wöste L., Bourayou R. and Saubrey R. (2004) Multiple Filamentation of Terawatt Laser in Laser, Phys. Rev. Lett., Vol. 92, No. 22, 225002, 4 p.
- [37] Trokhimchuck P. P. (2017) Problems of reradiation and reabsorption in Nonlinear and Relaxed Optics, IJARPS, Vol. 4, Is.2, 37-50
- [38] Kurilenko O. D. (1974) Short chemical handbook, Naukova Dumka, Kiev (In Russian)
- [39] Frank I. M. (1988) Cherenkov Radiation. Theoretical Aspects, Nauka, Moscow (In Russian)
- [40] Bohr N. (1950) The passage of charged particles through matter. IL, Moscow (In Russian)

Citation: Petro O. Kondratenko, (2019). *Problems of Modeling Diffraction and Interference Processes in Nonlinear and Relaxed Optics. International Journal of Advanced Research in Physical Science (IJARPS) 6(7), pp.5-17, 2019.*

Copyright: © 2019 Authors, This is an open-access article distributed under the terms of the Creative Commons Attribution License, which permits unrestricted use, distribution, and reproduction in any medium, provided the original author and source are credited.